Available online at www.sciencedirect.com

ScienceDirect

Procedia Engineering 140 (2016) 57 – 66

Procedia Engineering

www.elsevier.com/locate/procedia

MRS Singapore – ICMAT Symposia Proceedings

8th International Conference on Materials for Advanced Technologies

Enhancement of Labeled Alpha-fetoprotein Antibodies and Antigen-antibody Complexes Fluorescence with Silver Nanocolloids

Svetlana Vaschenko[a], Andrey Ramanenka[a]*, Olga Kulakovich[a], Alina Muravitskaya[a], Dmitry Guzatov[b], Anatoly Lunevich[c], Yuri Glukhov[c], Sergey Gaponenko[d]

[a]*B.I. Stepanov Institute of Physics of the National Academy of Sciences of Belarus, Nezavisimosti Avenue 68, Minsk 220072, Belarus*
[b]*P.N. Lebedev Physical Institute of the Russian Academy of Sciences, Leninskij Avenue 53, Moscow 119991, Russia*
[c]*ELTA Ltd., Aviatsionnaya Street 19/6, Moscow 123182, Russia*
[d]*EEE School, Nanyang Technological University, Nanyang Avenue 50, Singapore 639798, Singapore*

Abstract

A model immunoassay test system is proposed based on metal enhanced photoluminescence to analyze low concentrations of alpha-fetoprotein, a tumor marker. Antigen-antibody reaction was performed on polystyrene plates coated with silver nanoparticles to increase sensitivity of fluorescent immunoassay and signal-to-noise ratio as compared to silver-free system. The proposed test system model uses layer-by-layer assembly approach, LED excitation and nanowatt photodetection set-up, so it is characterized by smaller probe volume, fast analysis and simplicity. The proposed model system offers alpha-fetoprotein detection at concentrations used in clinical practice. Photostability and photoluminescence enhancement for labeled alpha-fetoprotein antibodies on a silver substrate were found to depend on antibodies concentration. Labeled antibodies photostability on substrates was found to deviate within 20 % as compared to silver-free samples whereas photoluminescence intensity enhancement is typically in the range of 6-8 times.

Selection and/or peer-review under responsibility of the scientific committee of Symposium 2015 ICMAT

Keywords: plasmon-enhanced fluorescence; silver nanoparticles; immunoassay; alpha-fetoprotein; poin-of-care testing

* Corresponding author. Tel.: +375-17-284-14-10; fax: +375-17-284-08-79.
E-mail address: a.ramanenka@ifanbel.bas-net.by

Selection and/or peer-review under responsibility of the scientific committee of Symposium 2015 ICMAT
doi:10.1016/j.proeng.2015.08.1111

1. Introduction

During last decades, much extensive studies have been performed worldwide to elaborate biophysical techniques for high-sensitive quantitative detection of biomolecules and their interactions. These studies are stimulated by existing demands in pharmacy, medical diagnostics, environment monitoring and in other fields. Accurate and fast protein detection in complex biological probes (blood, serum, saliva, milk etc.) is still important. These challenges stimulate interdisciplinary studies with potential outcome beyond the original tasks.

Quality and efficiency of immunoassays are closely connected with applied labels and their detection technique. For example, fluorescent detection techniques are typically more sensitive than photometric techniques by 1-2 orders of the magnitude [1]. Sensitivity of fluorescent immunoassay can be increased using plasmonically enhanced photoluminescence (PL). Depending on the original intrinsic quantum yield of the labels used, PL signal intensity can be raised up to 10…100 times if fluorescent molecules are placed near metal nanoparticles, typically golden or silver [2,3]. PL enhancement occurs as a result of positive balance between favorable local incident electromagnetic field enhancement, favorable radiative transition rate enhancement and undesirable metal induced quenching (non-radiative decay rate enhancement) [4,5]. Extensive studies towards practical application of metal enhanced fluorescence in immunoassay have been reported by many groups last decades [6-12].

We have recently demonstrated experimental implementation of metal enhanced fluorescence for model biomolecules, namely BSA-FITC (bovine serum albumin labeled with fluorescein isothiocyanate) [13-15] and human immunoglobulin IgG-FITC conjugates [16] on nanotextured silver films. We showed that the optimal size of silver nanoparticles for PL enhancement of FITC-containing conjugates is about 50 nm and optimized the fluorophore-metal spacing is a few nm. In the present paper, we report on application of metal enhanced fluorescence for detection of alpha-fetoprotein (AFP) using FITC-labeled antibodies. AFP is the known tumor marker indicating of liver cancer and some tumors in reproductive system. Its detection in blood at low levels is important for diagnostics and post-treatment monitoring. To date only a few works are known on plasmonics application for AFP immunoassay using surface plasmon resonance sensor [17,18], enhanced fluorescence [18-22] or enhanced Raman scattering [23]. However these approaches are rather expensive to be applied routinely in analytical practice because they need either expensive equipment (Kretschmann optical configuration with laser excitation via a prism [17,18,21,22], Raman instrumentation [23], or single-photon counting module for fluorescence correlation spectroscopy technique [20]) or complicated sample and probe preparation (electron beam evaporation technique for gold nanopatterned substrate fabrication [22]). To our knowledge, it has not been reported before about using silver colloidal films with plasmonic enhancement to sensitive detection of AFP.

In this paper, we evaluate the potential for low-level direct single-site fluorescent immunometric AFP detection [24,25] of a simple test system based on silver colloids plasmonically enhanced PL, fabricated using the simple electrostatic interaction of the components principle. The aim was to simplify both test-system preparation and the PL detection setup. Therefore all possible but expensive synthesis techniques for substrates were excluded (nanolithography, molecular beam epitaxy, chemical etching, vacuum deposition) and a commercial LED rather than a laser was used for PL excitation. Silver nanoparticles were deposited on the surface of cells in a standard commercial polystyrene array using polyelectrolyte layer-by-layer deposition technique. All other processes except for antigen-antibody conjugation were also based on electrostatic deposition. Special attention was paid to AFP concentration dependence of the PL signal which is important for quantitative analysis. We estimate the results presented in this work as significant steps towards rapid quantitative fluorescent immunoassay of AFP and other tumor markers for point-of-care testing.

2. Experimental

2.1. Materials

Silver nitrate, sodium citrate, poly(diallyldimethylammonium) chloride (PDADMAC; Mw = 200000 g/M), sodium chloride were all purchased from Sigma Aldrich. Other chemicals were fluorescein isothiocyanate (isomer I, Sigma), Tris-EDTA buffer solution (pH 7,6; Fisher BioReagents), albumin from bovine serum albumin (BSA, 98%, Aldrich), AFP in lyophilized form (Abcam).

Transparent polystyrene 96-well microplates with 380 µl well volume were purchased from Sarstedt AG & Co. (Germany).

2.2. Silver covering of polystyrene microplates

Silver sol was synthesized by $AgNO_3$ citrate reduction technique [26]. 9 mg of $AgNO_3$ was dissolved in 50 ml of water, and 1 ml of 1 % sodium citrate was added dropwise when the mixture began to boil. The reaction vessel was boiled for 20 min, ending with formation of yellow-brown sol.

Silver covering of polystyrene microplates was made as follows:

- 48 microwells (i.e. a half of 96-well microplate) were filled with 200 µl of PDADMAC (1 g/l in 0,5 M NaCl) for 20 min, then the plate was rinsed by distilled water.
- To deposit Ag nanoparticles, 200 µl of silver sol was added into microwells for 24 hrs and maintained at room temperature. After metallization the plate was rinsed by distilled water.
- 200 µl of PDADMAC (1 g/l in 0,5 M NaCl) was placed in all 96 microwells (both with silver, and without) for 20 min with the subsequent washing by distilled water. Thus, the top layer in all microwells was the layer of positively charged polyelectrolyte.

2.3. Preparation of the fluorescence probes

The synthesis of antiAFP-FITC conjugates (antiAFP means here and further AFP antibodies) was made according to standard procedure [27], the concentration of product is 2,97 mg/ml with antiAFP:FITC molar ratio 1:3,9. Working antiAFP-FITC solutions in a range of concentrations 0,5 – 40 µg/ml were obtained by dilution of as-prepared antiAFP-FITC by Tris-EDTA buffer. To examine metal enhanced fluorescence of antiAFP-FITC (see Fig. 1b), 100 µl aliquot was put both into metalized and pure microwells for 40 min at room temperature, then unbound antibody was washed off twice with Tris-EDTA buffer.

AFP*antiAFP-FITC complexes (the asterisk means specific binding between AFP and FITC-labeled antibody) were prepared directly in microwells as described below (see also Fig. 1c). Every stage of this procedure was performed at 20 ºC.

- 100 µl aliquot of working AFP solutions (0,005-40 µg/ml) was put both into metallized and pure microwells for 40 min. Rinsing by Tris-EDTA buffer was performed after incubation.
- Before application of labeled antibody, possible non-specific binding sites were blocked by adding of 100 µl 1 % BSA solution for 20 min. Excess of BSA was washed off by Tris-EDTA buffer.
- 100 µl aliquot of antiAFP-FITC (10 µg/ml) was added in each microwell and left for 1 hr for immunoreaction. Unbound labeled antibody was washed off with Tris-EDTA buffer. Finally, microwells were dried and measured.

Thus, the method included direct determination of AFP by immunoreaction of AFP and labeled antiAFP in a one-step process.

2.4. Measurements

Atomic force microscopy (AFM) images of silver films were taken in air using NT-206 device (Microtestmachines, Belarus). Measurements were made in a contact mode using 0,03 N/m CSC38B probes.

Optical density spectra in the range of 300 to 800 nm were measured using a Cary-500 spectrophotometer (Varian, USA). Luminescence spectra were measured using a home-made spectrometer based on S-3801 spectrograph (Solar TII, Belarus) with a 150 grooves/mm grating and a liquid nitrogen cooled silicon CCD camera LN-CCD-1152-E PROD FG (Princeton Instruments, USA). A light emitting diode (LED) ARPL-3W Blue (Arlight, Russia) was used as the excitation light source with emission maximum at 460 nm and spectral half-width ~25 nm. Excitation radiation as well as fluorescence registration has been performed in a direction normal to the sample surface (Fig. 1a) using an Olympus LMPlanFl microscope objective. All measurements were done at room temperature. Fluorescence spectra were not corrected to account for the spectral response of detecting system.

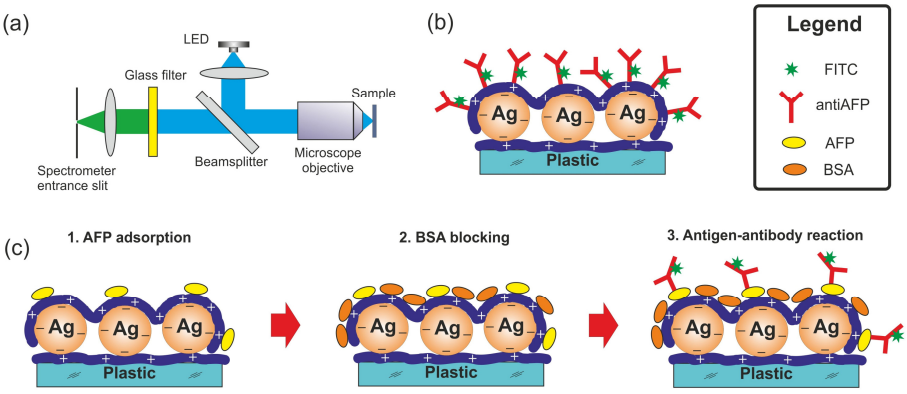

Fig. 1. (a) Experimental setup of fluorescence registration system. (b) Experimental plasmonic samples with adsorbed antiAFP-FITC for evaluation of plasmonic fluorescence enhancement feasibility. (c) AFP immunoassay procedure.

3. Results and Discussion

3.1. Characterization of Ag-coated microwells for plasmonic fluorescence enhancement

The SEM image of silver sol (not shown here; see Ref. 14) as well as AFM data of Ag nanoparticles deposited on PDADMAC-modified polystyrene microwells (Fig. 2a) show nearly continuous layer of spherical Ag nanoparticles with diameter from 30 to 80 nm. The sufficiently even nanoparticle covering was observed. That means the process of colloidal Ag film formation on polystyrene microwells seems to be the similar to the process on the PDADMAC-modified glass surface [14].

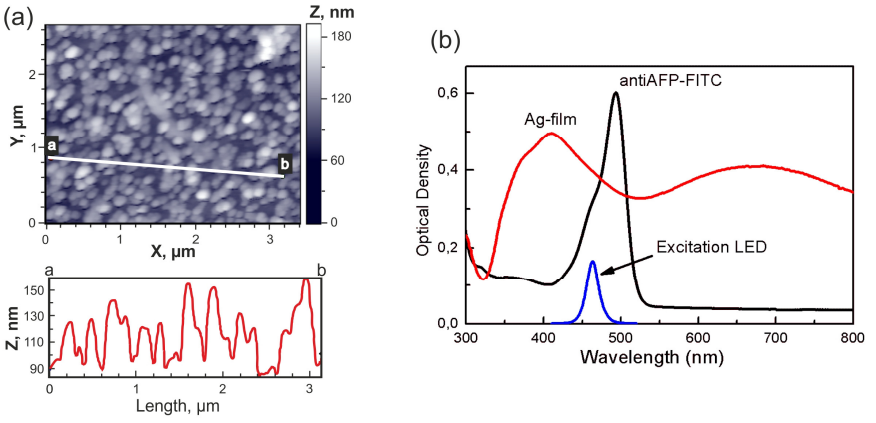

Fig. 2. (a) Typical AFM image and surface profile of a polystyrene microwell covered with silver nanoparticles. (b) Optical density spectra of Ag-coated polystyrene microwells and antiAFP-FITC solution. The LED emission spectrum is also shown (in arbitrary units).

The optical density spectrum of a substrate containing silver nanoparticles features a maximum near 400 nm as well as the broad 600-800 nm band (Fig. 2b). The first band corresponds to well-known silver nanoparticles surface plasmon absorption while the second belongs to the absorption of silver particle aggregates. These are known to give higher local incident field enhancement [28] which is very desirable in metal enhanced fluorescence techniques. Optical density spectra of Ag-coated polystyrene and Ag-coated glass (the latter were studied in Ref. 14) as well as their AFM images show the similarity of these types of Ag colloidal films.

Since the absorption band of antiAFP-FITC (antiAFP doesn't absorb light in visible spectral range) overlaps with the film absorption band defined by the surface plasmon resonance, one may expect the effective FITC excitation and antiAFP-FITC fluorescence enhancement [29,30].

As it was observed earlier, the maximal fluorescence enhancement factor in the "BSA-FITC on silver colloidal films" model systems was found to occur for distances between silver and labeled molecules corresponding to 1-3 polyelectrolyte layers [13-15]. So, in this work antiAFP-FITC was adsorbed atop the 1 polyelectrolyte layer. This is the minimum spacer thickness provided by the current technique and accords to 1,4 nm [31]. Schematic illustration of microwell surfaces for antiAFP and AFP detection is shown in Fig. 1b and Fig. 1c.

3.2. Fluorescence enhancement of antiAFP-FITC in Ag-coated polysterene microwells

To study the possibility of using Ag-coated microwells (see Fig. 1b) for quantitative AFP fluorescent immunoassay we investigated the dependence of PL signal on the fluorescent label (antiAFP-FITC) concentration (see Fig. 3). PL enhancement factor (Fig. 3, the inset) was calculated as the ratio between fluorescence intensity of antiAFP-FITC adsorbed from the equal solution concentration on the Ag-coated and uncoated polystyrene microwells. PL intensity was determined in maximum (530 nm).

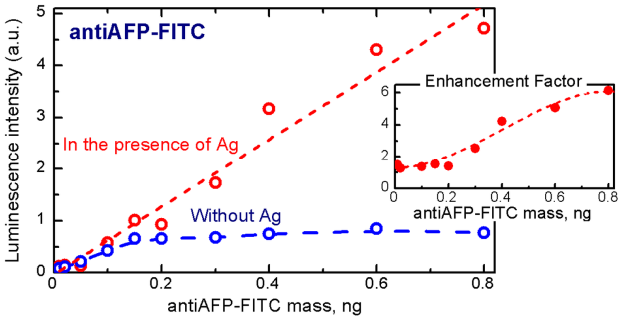

Fig. 3. The dependence of PL intensity of antiAFP-FITC on its amount in the presence and in the absence of Ag nanoparticles. Mass of antiAFP-FITC under detection (X axis) is estimated given antiAFP-FITC fraction adsorbed on microwell bottom surface from its solution as well as light illuminated detection surface area. The inset shows the calculated dependence for PL enhancement factor.

The increase in PL intensity with increasing concentration was observed for labeled antibodies adsorbed on silver films, whereas the PL intensity dependence of antiAFP-FITC on the control plastic substrates reach the rapid saturation (Fig. 3). Thus, the increase in the antiAFP-FITC PL enhancement factor with increasing the analyte concentrations occurs in the presence of silver nanoparticles (the inset in Fig. 3).

Such a dependence has been described previously [12] for model assay system (polyclonal human IgG – goat antihuman IgG labeled with near-infrared dye Cy5) on 149 nm Ag-particles. Probably, a higher value of the PL enhancement factor for Cy5 was observed due to the low quantum yield of photoluminescence (0,28) compared with FITC (0,92). In other words, besides a local increase of the electromagnetic field near the metal, the changing in the fluorophore radiative and non-radiative decay rates may occur [4,14]. Therefore, it is possible to achieve higher enhancement values for a low quantum yield probes. Regardless of the PL quantum yield value there is no PL concentration quenching of labels adsorbed on silver substrates due to Forster resonance energy transfer as it is typical for labels on dielectric substrates. A similar behavior of the concentration quenching in the presence of silver has been previously described for human serum albumin (HSA) labeled with FITC. Increasing in the number of FITC-labels per HSA molecule from 1 to 7 led to 4-fold increasing the PL enhancement factor [32]. In our case (~3,9 FITC molecules per one antiAFP molecule) the PL concentration quenching should be also influenced by interaction of adjacent antiAFP-FITC molecules adsorbed on the surface clusters of polycation charges [33].

Fig. 3 shows that the presence of Ag nanoparticles increases PL intensity by 1,5 times for low label concentrations and up to 6 times for high antiAFP-FITC concentrations.

Notably, the continuous fluorescence light power in the course of the above experiments measured by the detection system was about 0,4 nW for 1 ng of antiAFP-FITC. This means the cheap silicon non-cooled detector can be successfully applied that makes the approach promising for routine fluotesters development.

3.3. AFP immunoassay in Ag-coated polystyrene microwells

After successful validation of fluorescence plasmonic enhancement for labeled antibodies, direct immunometric assay for AFP detection was performed (immunoassay scheme see in Fig. 1c). Fig. 4a shows the PL spectra of AFP*antiAFP-FITC complexes, obtained after the antigen-antibody reaction held on the surface of plastic and Ag-coated microwells. The data presented shows that the metal induced PL enhancement persists also for conjugates. The PL enhancement factor for "AFP*antiAFP-FITC" on silver film as compared with a plastic substrate is about 8, i.e., this value is higher than for antiAFP-FITC. This discrepancy is probably due to the additional layer of AFP and BSA molecules between the metal and the FITC label which optimizes the "metal – fluorophore" spacing and produces more favorable conditions for plasmon-enhanced PL.

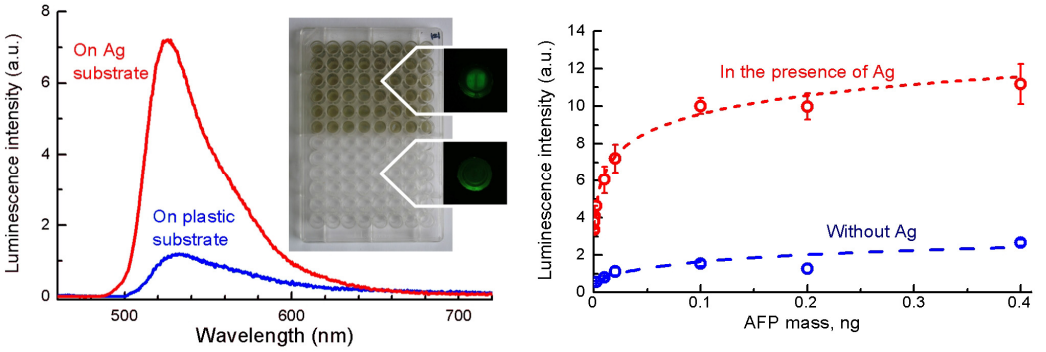

Fig. 4. (a) Photoluminescence spectra of «AFP*antiAFP-FITC» complexes on the surface of Ag-coated and uncoated plastic microwells. Spectra presented is referred to microwells with AFP mass under detection equal to 0,02 ng. (b) Photoluminescence intensity dependence on AFP concentration (mass). AFP mass under detection (X axis) is estimated given AFP fraction adsorbed on microwell bottom surface from its solution as well as light illuminated detection surface area.

It should be noted that in both cases, the presence of Ag film provides increasing of the PL signal/noise ratio. AFP in silver microwells was traced when adsorbed even from 5 ng/ml solution. The concentration of AFP in human plasma is nearly 10 ng/ml for healthy people, but this level increases markedly (to nearly 1 μg/ml and higher [17,22,34,35]) when patients carry hepatocellular or some other types of cancer. Thus, sensitivity of the proposed direct immunoassay model system is at the clinical diagnosis level.

3.4. Fluorescence enhancement/quenching theoretical modeling

Recently we proposed the theoretical model of fluorescence enhancement/quenching for fluorophores near spherical metal nanoparticles [14]. In this model fluorophores are treated as dipoles and 'single fluorophore – single silver nanoparticle' system is considered. The approach takes into account simultaneously local intensity enhancement, radiative and nonradiative rates modification in the close vicinity of silver nanoparticles, and also excitation light polarization, silver nanoparticle size, fluorophore position, and its dipole moment orientation.

Fig. 5 shows calculated PL enhancement factor dependence on both excitation wavelength and fluorophore-silver nanoparticle spacing. The calculations performed correspond to our experimental conditions: emission wavelength was chosen equal to 530 nm (FITC), enhancement factor was averaged on silver nanoparticle size for nanoparticles ensemble with Gaussian distribution (mean diameter 47 nm and dispersion 30 nm).

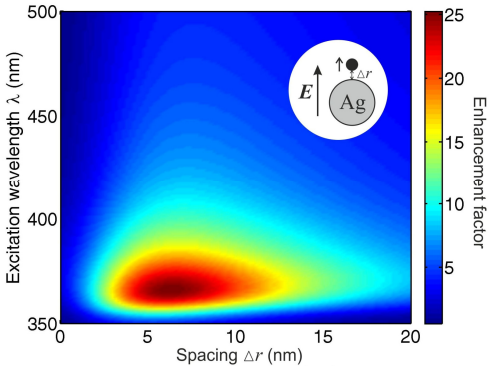

Fig. 5. Calculated weighted luminescence enhancement factor versus excitation wavelength and fluorophore-silver nanoparticle spacing Δr with averaging over ensemble of silver nanoparticles with Gaussian distribution (mean diameter 47 nm and dispersion 30 nm). The insert shows the geometry of the model: arrows indicate that the fluorophore dipole moment is normal to a silver particle surface and is parallel to the electric field ***E*** of the excitation light.

As seen from Fig. 5, maximal PL enhancement factor is predicted for excitation wavelength range 360..380 nm and «fluorophore – silver nanoparticle» spacing Δr equal to 4..11 nm. In practice, excitation wavelength range 360..380 nm is insufficient due to low FITC absorption in this spectral range (see Fig. 2b). For LED excitation used in our experiment (440..490 nm, see also Fig. 2b) and spacing Δr equal to some nanometers predicted PL enhancement factor is about 5 times. As was mentioned above in Sections 3.2, 3.3 experimental PL enhancement factor was up to 6 times for antiAFP-FITC and was about 8 times for AFP*antiAFP-FITC complexes, and this enhancement difference was attributed to increased spacing between FITC and silver nanoparticles. One can see the theoretical calculations prove this statement (PL enhancement distance dependence for chosen excitation wavelength is more clear for maximal enhancement area corresponding to e.g. 370 nm). Nevertheless it should be noted that proposed theoretical model describes only a quite simple model and experimental case is more complicated. It includes unpolarized LED excitation with wide spectrum, partial silver nanoparticles aggregation (dimers and many nanoparticles effects), and possible random orientations of FITC dipole moments relative to silver nanoparticles surface.

3.5. Photostability measurements

Fig. 6 shows the dependence of the PL intensity on LED exposition time for antiAFP-FITC deposited on silver and plastic substrates for microwells with antiAFP-FITC amount under detection equal to 0,4 ng and 0,8 ng correspondingly. One can observe the increasing of the antiAFP-FITC photostability in the presence of silver with increasing the analyte concentration while photostability for plastic substrates remains the same.

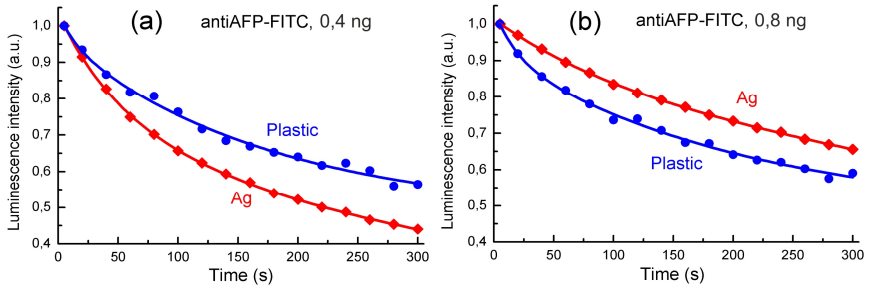

Fig. 6. Normalized fluorescence intensity of antiAFP-FITC as a function of time on Ag-coated and uncoated microwells for different amounts of analyte under detection: (a) 0,4 ng, (b) 0,8 ng. Excitation wavelength is 460 nm, emission wavelength is 530 nm.

Fluorophore photobleaching on plastic surface can be described by simple mechanism of fluorophore photochemical reaction with molecular oxygen from fluorophore long-lived triplet excited state [36]. This process shouldn't be affected by concentration in our case of sparse packing of fluorophores on plastic surface.

In case of fluorophores deposited on noble metal surface the situation is changed drastically. Main photobleaching mechanism remains the same (photochemical reaction with molecular oxygen). But in the close vicinity of metal parameters of this mechanism can be changed significantly: fluorophore excitation rate is increased by local enhanced electromagnetic field as well as fluorophore radiative decay rate is increased too (fluorophore excited state lifetime is shortened) [37]. As a result, fluorophore molecule near metal surface will stay in the excited state for a shorter time, but the number of excitation-emission cycles will be larger. So, assuming that PL degradation happens from the excited state, one can observe either reducing [38] or rising [39] of fluorophore photobleaching in the presence of metal, depending on which mechanism prevails. These effects also can lead probably to dependence of the rate of photodegradation on fluorophore–metal spacing, fluorescence quantum yield and other factors.

But concentration dependence of antiAFP-FITC photostability for metal substrates can be described only with additional, ensemble-based mechanism. Explanation can be as follows. Fluorescein-based dyes (e.g. FITC) are subjects to significant thermal degradation at elevated temperatures [40]. Silver nanoparticles (especially many particle systems) can be the effective heating source of surrounding media [41]. For silver nanoparticles deposited on a substrate the distribution of heat sources can be highly nonuniform with formation of so-called thermal hot spots [42]. So, one can assume that for low analyte concentrations antiAFP-FITC is deposited mainly in thermal hot spots and with concentration increasing the majority of thermal hot spots is already occupied and antiAFP-FITC is deposited in other places. As a consequence, for low concentrations ensemble-averaged photostability is determined by negative metal influence (FITC thermal degradation in thermal hot spots resulted in averaged lower photostability), but with concentration increasing ensemble-averaged photostability is determined by positive metal influence (we assume that excitation state lifetime shortening prevails over larger number of excitation-emission cycles resulted in averaged greater photostability).

4. Conclusion

Plasmon-enhanced fluorescence for FITC-labeled AFP antibodies and labeled antibody-antigen AFP complexes has been investigated for nanostructures based on colloidal silver nanoparticles deposited on polystyrene substrates. Plasmonic substrates were fabricated using a simple bottom-up layer-by-layer approach of electrostatic interaction of components. The two stage preparation technique of silver films on plastic substrates has been elaborated by means of colloidal chemistry. Optical scheme was simplified by using cheap commercial LED as fluorescence excitation source.

It has been demonstrated the possibility of AFP low quantities detection well below 0.1 ng, corresponding to concentration levels typical for clinical practice. Fluorescence signal was enhanced by up to 6 times for AFP antibodies and by 8 times for AFP complexes using silver nanoparticles covered substrates in comparison to uncovered polystyrene substrates.

Both photoluminescence intensity enhancement factor and photoluminescence stability upon illumination time rise up with analyte concentration increasing. Even in cases when metal proximity makes photostability somewhat lower, the detection limit remains considerably improved owing to higher enhancement in luminescence intensity.

The detected light power was about 1 nW per 1 ng that means the cheap silicon non-cooled detector can be successfully applied in fluotesters. The results show that solid state metal-enhanced spectroscopy offers a promising way for clinical diagnostics for direct rapid quantitative immunoassays.

Acknowledgements

The authors acknowledge helpful discussions with Dr. V.A. Goranov and synthesis of antiAFP-FITC conjugates by S.N. Gilevich (Institute of Bioorganic Chemistry, National Academy of Sciences of Belarus). The work has been supported by the National Program "Convergence" and by the "ELTA Ltd" (Russia).

References

[1] A.J. Ozinskas, Principles of Fluorescence Immunoassay, in: J.R. Lakowicz (Ed.), Topics in Fluorescence Spectroscopy, Volume 4: Probe Design and Chemical Sensing, Plenum Press, New York, 1994, pp. 449–496.

[2] D.A. Weitz, S. Garoff, J.I. Gersten, A. Nitzan, The enhancement of Raman scattering, resonance Raman scattering, and fluorescence from molecules adsorbed on a rough silver surface, J. Chem. Phys. 78 (1983) 5324–5338.

[3] J. Kümmerlen, A. Leitner, H. Brunner, F.R. Aussenegg, A. Wokaun, Enhanced dye fluorescence over silver island films: analysis of the distance dependence, Mol. Phys. 80 (1993) 1031–1046.

[4] S.V. Gaponenko, Introduction to Nanophotonics, Cambridge University Press, Cambridge, 2010.

[5] C.D. Geddes, Ed., Metal-Enhanced Fluorescence, Wiley, Hoboken (USA), 2010.

[6] J.W. Attridge, P.B. Daniels, J.K. Deacon, G.A. Robinson, G.P. Davidson, Sensitivity enhancement of optical immunosensors by the use of a surface plasmon resonance fluoroimmunoassay, Biosens. Bioelectron. 6 (1991) 201–214.

[7] F. Yu, B. Persson, S. Löfås, W. Knoll, Surface plasmon fluorescence immunoassay of free prostate-specific antigen in human plasma at the femtomolar level, Anal. Chem. 76 (2004) 6765–6770.

[8] K. Sokolov, G. Chumanov, T.M. Cotton, Enhancement of molecular fluorescence near the surface of colloidal metal films, Anal. Chem. 70 (1998) 3898–3905.

[9] S.M. Tabakman, L. Lau, J.T. Robinson, J. Price, S.P. Sherlock, H. Wang, B. Zhang, Z. Chen, S. Tangsombatvisit, J.A. Jarrell, P.J. Utz, H. Dai, Plasmonic substrates for multiplexed protein microarrays with femtomolar sensitivity and broad dynamic range, Nat. Commun. 2 (2011) 466.

[10] L. Zhou, F. Ding, H. Chen, W. Ding, W. Zhang, S.Y. Chou, Enhancement of immunoassay's fluorescence and detection sensitivity using three-dimensional plasmonic nano-antenna-dots array, Anal. Chem. 84 (2012) 4489–4495.

[11] R. Zhang, Z. Wang, C. Song, J. Yang, Y. Cui, A straightforward immunoassay applicable to a wide range of antibodies based on surface enhanced fluorescence, J. Fluoresc. 23 (2013) 551–559.

[12] R. Nooney, A. Clifford, X. LeGuevel, O. Stranik, C. McDonagh, B.D. MacCraith, Enhancing the analytical performance of immunoassays that employ metal-enhanced fluorescence, Anal. Bioanal. Chem. 396 (2010) 1127–1134.

[13] O. Kulakovich, N. Strekal, M. Artemyev, S. Stupak, S. Maskevich, S. Gaponenko, Improved method for fluorophore deposition atop a polyelectrolyte spacer for quantitative study of distance-dependent plasmon-assisted luminescence, Nanotechnology 17 (2006) 5201–5206.

[14] D.V. Guzatov, S.V. Vaschenko, V.V. Stankevich, A.Ya. Lunevich, Y.F. Glukhov, S.V. Gaponenko, Plasmonic enhancement of molecular fluorescence near silver nanoparticles: theory, modeling, and experiment, J. Phys. Chem. C 116 (2012) 10723–10733.

[15] S.V. Vaschenko, A.A. Ramanenka, D.V. Guzatov, V.V. Stankevich, A.Ya. Lunevich, Y.F. Glukhov, I.F. Sveklo, S.V. Gaponenko, Plasmon-enhanced fluorescence of labeled biomolecules on top of a silver sol-gel film, J. Nanophoton. 6 (2012) 61710.

[16] A.A. Ramanenka, S.V. Vaschenko, V.V. Stankevich, A.Ya. Lunevich, Y.F. Glukhov, S.V. Gaponenko, Plasmonic enhancement of luminescence of fluorescein isothiocyanate and human immunoglobulin conjugates, J. Appl. Spectrosc. 81 (2014) 222–225.

[17] Y. Teramura, H. Iwata, Label-free immunosensing for α-fetoprotein in human plasma using surface plasmon resonance, Anal. Biochem. 365 (2007) 201–207.

[18] Y. Arima, Y. Teramura, H. Takiguchi, K. Kawano, H. Kotera, H. Iwata, Surface Plasmon Resonance and Surface Plasmon Field-Enhanced Fluorescence Spectroscopy for Sensitive Detection of Tumor Markers, in A. Rasooly, K.E. Herold (Eds.), Methods in Molecular Biology: Biosensors and Biodetection, Volume 503, Humana Press, New York, 2009, pp. 3–20.

[19] Y.-F. Chang, R.C. Chen, Y.J. Lee, S.C. Chao, L.C. Su, Y.C. Li, C. Chou, Localized surface plasmon coupled fluorescence fiber-optic biosensor for alpha-fetoprotein detection in human serum, Biosens. Bioelectron. 24 (2009) 1610–1614.

[20] L. Tang, C. Dong, J. Ren, Highly sensitive homogenous immunoassay of cancer biomarker using silver nanoparticles enhanced fluorescence correlation spectroscopy, Talanta 81 (2010) 1560–1567.

[21] T. Murakami, Y. Arima, M. Toda, H. Takiguchi, H. Iwata, Effect of dielectric spacer thickness on signal intensity of surface plasmon field-enhanced fluorescence spectroscopy, Anal. Biochem. 421 (2012) 632–639.

[22] S. Lee, S.H. Kang, Single-Molecule Sandwich Immunoassay for Quantification of Alpha-Fetoprotein Based on Evanescent Field-Enhanced Fluorescence Imaging, J. of Nanomaterials 2012 (2012) Article No. 4.

[23] J.-L. Gong, Y. Liang, Y. Huang, J.W. Chen, J.H. Jiang, G.L. Shen, R.Q. Yu, Ag/SiO_2 core-shell nanoparticle-based surface-enhanced Raman probes for immunoassay of cancer marker using silica-coated magnetic nanoparticles as separation tools, Biosens. Bioelectron. 22 (2007) 1501–1507.

[24] C. Davies, Principles of Competitive and Immunometric Assays (Including ELISA), in D. Wild (Ed.), The Immunoassay Handbook (4th edition), Elsevier, Oxford, 2013, pp. 29-59.

[25] C. Nistor, J. Emnéus, Immunoassay: Potentials and Limitations, in L. Gorton (Ed.), Biosensors and Modern Biospecific Analytical Techniques, Elsevier, Amsterdam, 2005, pp. 375-427.

[26] J. Fang, C. Zhong, R. Mu, The study of deposited silver particulate films by simple method for efficient SERS, Chem. Phys. Lett. 401 (2005) 271−275.

[27] N. Nakamura, T.K. Lim, J.M. Jeong, T. Matsunaga, Flow immunoassay for detection of human chorionic gonadotrophin using a cation exchange resin packed capillary column, Anal. Chim. Acta 439 (2001) 125–130.

[28] Z.B. Wang, B.S. Luk'yanchuk, W. Guo, S.P. Edwardson, D.J. Whitehead, L. Li, Z. Liu, K.G. Watkins, The influences of particle number on hot spots in strongly coupled metal nanoparticles chain, J. Chem. Phys. 128 (2008) 094705.

[29] N. Strekal, A. Maskevich, S. Maskevich, J.C. Jardillier, I. Nabiev, Selective enhancement of Raman or fluorescence spectra of biomolecules using specifically annealed thick gold films, Biopolymers (Biospectroscopy) 57 (2000) 325–328.
[30] O. Kulakovich, N. Strekal, A. Yaroshevich, S. Maskevich, S. Gaponenko, I. Nabiev, U. Woggon, M. Artemyev, Enhanced luminescence of CdSe quantum dots on gold colloids, Nano Lett. 2 (2002) 1449–1452.
[31] F. Caruso, Nanoengineering of particle surfaces, Adv. Mater. 13 (2001) 11–22.
[32] J.R. Lakowicz, J. Malicka, S. D'Auria, I. Gryczynski, Release of the self-quenching of fluorescence near silver metallic surfaces, Anal. Biochem. 320 (2003) 13–20.
[33] F. Caruso, H. Lichtenfeld, E. Donath, H. Möhwald, Investigation of Electrostatic Interactions in Polyelectrolyte Multilayer Films: Binding of Anionic Fluorescent Probes to Layers Assembled onto Colloids, Macromolecules 32 (1999) 2317–2328.
[34] K. Okuda, Early recognition of hepatocellular carcinoma, Hepatology 6 (1986) 729–738.
[35] K. Okuda, Primary liver cancer, Digest. Dis. Sci. 31 (1986) 133S–146S.
[36] L. Song, C.A. Varma, J.W. Verhoeven, H.J. Tanke, Influence of the triplet excited state on the photobleaching kinetics of fluorescein in microscopy, Biophys. J., 70 (1996) 2959–2968.
[37] K. Vasilev, F.D. Stefani, V. Jacobsen, W. Knoll, M. Kreiter, Reduced photobleaching of chromophores close to a metal surface, J. Chem. Phys. 120 (2004) 6701–6704.
[38] C.D. Geddes, A. Parfenov, D. Roll, I. Gryczynski, J. Malicka, J.R. Lakowicz, Silver fractal-like structures for metal-enhanced fluorescence: enhanced fluorescence intensities and increased probe photostabilities, J. Fluoresc. 13 (2003) 267–276.
[39] C.D. Geddes, H. Cao, I. Gryczynski, Z. Gryczynski, J.R. Lakowicz, Metal-enhanced fluorescence (MEF) due to silver colloid on a planar surface: Potential applications of indocyanine green to in vivo imaging, J. Phys. Chem. A 107 (2003) 3443–3449.
[40] M.C. Adams, J. Davis, Kinetics of fluorescein decay and its application as a geothermal tracer, Geothermics 20 (1991) 53–66.
[41] G. Baffou, R. Quidant, Thermo-plasmonics: using metallic nanostructures as nano-sources of heat, Laser Photonics Rev. 7 (2013) 171–187.
[42] G. Baffou, C. Girard, R. Quidant, Mapping Heat Origin in Plasmonic Structures, Phys. Rev. Lett. 104 (2010) 136805.